SAXS and SANS Studies of Surfactants and Reverse Micelles in Supercritical CO_2 [1]

J. D. Londono[2], R. S. Dharmapurikar[2], G. D. Wignall[2] and H. D. Cochran[2,3],

---

1. Paper presented at the Thirteenth Symposium on Thermophysical Properties, June 22-27, 1997, Boulder, CO, USA.

2. Oak Ridge National Laboratory, P.O. Box 2008, Oak Ridge, TN 37831-6224 (USA).

3. To whom correspondence should be addressed.

ABSTRACT

Surfactants promise to extend the applicability of supercritical CO_2 (SC-CO_2) to processing of insoluble materials such as polymers and aqueous systems. Important surfactant developments by DeSimone at the University of North Carolina and by Beckman at the University of Pittsburgh are being investigated at Oak Ridge National Laboratory at a fundamental, microscopic level using small angle x-ray and neutron scattering (SAXS and SANS) techniques. These experiments, with both surfactant solutions and microdispersions in SC-CO_2, enable us to determine the radius of gyration (R_g) and molecular weight (MW) of polymeric surfactant molecules in solution; the second osmotic virial coefficient (A_2) which characterizes the solvent-surfactant interaction in solution; and the shape and size of reverse micelles in solution. With DeSimone's group, we have studied solutions of poly(1,1-dihydro perfluoro octyl acrylate) (PFOA) in SC-CO_2 via SANS, first quantifying R_g, then MW, giving $R_g/(MW)^{1/2} = 0.1 \pm 0.03$[Å $g^{-1/2}$] and, by varying concentration, $A_2 \propto MW^{-0.4}$. These results quantify the basis for the SC-CO_2-philic fluoropolymer surfactant tail and show that the form of the variations observed was similar to those previously observed for conventional surfactant systems. DeSimone's group has shown that PFOA-b-polystyrene (PFOA-b-PS) block copolymers are useful as surfactants for the heterogeneous polymerization of PS. PFOA-b-PS copolymers were studied via SAXS and SANS. Spherical aggregates with aggregation number ($N_{agg} = 6-7$) were observed to be independent of the (CO_2-philic) PFOA block length, at constant PS block length, in accord with theory. The micelle cores were observed to swell from about 30 Å to about 50 Å in radius on addition of styrene (relatively insoluble in SC-CO_2) demonstrating the technological potential of surfactant-modified SC-CO_2 systems. Increase of pressure leads to smaller, more polydisperse aggregates, suggesting a critical micelle density. In continuing work, perfluoro polyether and other surfactants from Beckman's group and additional systems from DeSimone's group are being studied. Complementary molecular simulations, using ORNL's massively parallel Intel Paragon supercomputers, are also being undertaken.

Key Words: neutron scattering, reverse micelles, supercritical CO_2, surfactants, x-ray scattering

1. INTRODUCTION

In this short paper we will summarize the techniques for studying surfactants and reverse micelles in SC-CO_2 using SAXS and SANS; we will describe the scattering instruments and the pressure cells for conducting these studies; we will describe the types of measurement that yield the desired characterizations; we will describe the methods of data analysis and interpretation; and we will provide illustrative results from our laboratory.

2. APPARATUS

2.1 10 m SAXS Facility at ORNL.

The 10 m SAXS camera [1] constructed at ORNL was the first point-geometry camera equipped with a two-dimensional detector, allowing measurement of a true scattering pattern, virtually free from the need for collimation (desmearing) corrections. The instrument is available for use by external scientists as a user facility. The camera utilizes graphite-monochromatized Cu K_α or Mo K_α radiation (Cu K_α with $\lambda = 1.54\text{Å}$ was used in this study), with two-slit collimation and a third (guard) slit positioned close to the sample as shown in Figure 1. Parasitic scattering is substantially reduced by this configuration providing excellent performance down to a scattering vector $Q = 4\pi\lambda^{-1}\sin\theta \approx 3 \text{ x } 10^{-3}\text{A}^{-1}$, where λ is the wavelength and 2θ is the angle of scatter [2].

2.2 SAXS Pressure Cell.

Figure 2 shows the SAXS pressure cell which was designed after one by Fulton *et al.* [3]. Key to the performance of this cell are the two 1 mm thick single crystal diamond windows that are brazed into nuts which screw into the monoblock stainless steel cell body.

2.3 30-m SANS Facility at ORNL.

This instrument uses a pinhole geometry with collimating slits of 0.5-3.5 cm dia. separated by a distance of 10 m [4]. The beam may be transported to distances of 1.5, 3.5 or 7.5 m from the sample by means of movable neutron guides. The 64 by 64 cm area detector has 1.0 by 1.0 cm resolution elements and can be positioned at any distance from 1.5 to 19 m

from the specimen in an evacuated flight path. The standard incident wavelength provided by a bank of pyrolytic graphite crystals, is 4.75 Å, though this can be changed to 2.38 Å by substituting graphite for the cold beryllium filter normally in position. This gives a Q-range of 0.003 to 0.75 A^{-1}, and the instrument is capable of resolving scattering from particles containing as few as 60 atoms. [4] All data may be converted to an absolute (±3%) differential cross section per unit sample volume (in units of cm^{-1}) by comparison with pre-calibrated secondary standards [5]. The detector efficiency calibration is based on the scattering from light water and this leads to angle-independent scattering for vanadium, H-polymer blanks and water samples of different thicknesses in the range 1-10 mm.

2.4 SANS Pressure Cell.

Figure 3 shows the SANS pressure cell; the sapphire windows and spacers have good neutron transmission characteristics, >80% with maximum number of spacers. The electrically-heated monoblock cell body can be disassembled and cleaned with ease.

3. METHODS AND ILLUSTRATIVE RESULTS

3.1 Surfactant Solutions.

Figure 4 is a Zimm plot of the inverse of the absolute scattering intensity, $I(Q) = d\,\Sigma/d\,\Omega$, called the differential scattering cross section (in units of cm^{-1}), versus the scattering vector squared from a SANS experiment on a 10 w/v% solution in SC-CO_2 of high (but at the time unknown) molecular weight poly(1,1-dihydro perfluoro octyl acrylate) (PFOA), produced by DeSimone's group, measured at approximately 338 K and 34.5 MPa. Three measurements were needed to determine $I(Q)$—a run with the cell filled with CO_2 but no PFOA, a run with the sample-filled cell, and a calibration run—and the total beam time was approximately 6 to 8 hours. The Zimm plot allows reliable extrapolation to $Q = 0$. The radius of gyration (R_g) of the PFOA chains in solution at this condition is given by the square root of three times ratio of slope to intercept; in this case R_g = 100±9 Å.

Figure 5 shows further analysis of the results of a number of measurements like those shown in Figure 4 covering a range of surfactant concentrations. The inverse of the differential cross section at $Q = 0$ times the PFOA concentration, c, times the known contrast factor, K, is plotted against c for the high molecular weight PFOA and a low molecular weight PFOA. The contrast factor, K, is given by $K = [\Delta SLD]^2/\rho_p N_0$, where SLD is the scattering length density, ρ_p is the PFOA density, and N_0 is Avogadro's number. For the PFOA, $SLD = 0.0336 \times 10^{12}$ cm^{-2}, and for the CO_2, $SLD = \rho_{CO_2} \times 2.498 \times 10^{-2}$ cm^{-2}. The inverse of the intercept of the fitted lines at $c = 0$ gives the molecular weight (MW) and the slope is twice the second osmotic virial coefficient (A_2), a measure of the affinity of the PFOA for SC-CO_2. Table I shows the results. From these results we find $A_2 \propto MW^{-0.4}$ and $R_g/(MW)^{1/2} = 0.1 \pm 0.03$ [A g$^{-1/2}$], variations that are similar to those found for polymer solutions in liquid solvents.

Figure 6 shows how $[d\Sigma/d\Omega(0)]^{-1}$ varies with CO_2 pressure for the high MW PFOA at 3 w/v% and 338K, indicating the solubility limit the PFOA to be about 30.1 MPa (4360 psi).

3.2 Reverse Micelles.

When graft copolymers are formed from PFOA and a second polymer such as poly(ethylene oxide) (PEO), the resulting molecules are useful surfactants that can form reverse micelles in SC-CO_2 that can support a medium in their cores which would be otherwise insoluble in SC-CO_2 [7,8]. Fulton and co-workers [3] first studied water-swollen PFOA-g-PEO reverse micelles in SC-CO_2 using SAXS. The characteristics of the reverse micelles can be determined by fitting the data to a core-shell model [7]. To quantify and refine the earlier results, we performed SANS studies of PFOA-g-PEO swelled with H_2O and swelled with D_2O and compared the results with a simulation based on the parameters reported previously [3]. Figure 7 illustrates the power of isotope substitution in SANS experiments to vary the contrast (ΔSLD) of one component in a complex system and also illustrates that even an approximate calibration (±25%) can avoid such discrepancies.

Independently calibrated SAXS and SANS data [9] can provide strong confirmation of the quantitative characterization of micellar systems. Figure 8 shows the fits of the core-shell model to SAXS and SANS data for reverse micelles formed from block a copolymers of poly(styrene) (PS) with PFOA. It is evident from the figure that the SAXS results for this system benefit (by better than an order of magnitude) from the larger $(\Delta SLD)^2$ for PFOA in SC-CO_2. Our research efficiency and flexibility are improved by using SAXS and SANS once quantitative characterization of a micellar system has been confirmed. When styrene oligomer (average degree of polymerization $N = 5$) was added to the micellar dispersion of PFOA-b-PS in SC-CO_2, almost all was contained within the core of the micelles, both the core radius (R_i) and the aggregation number ($N_{agg} =$ number of PFOA-b-PS surfactant molecules per micelle) increasing to accommodate the added oligomer. Figure 9 shows typical results for a dispersion of 4.0 w/v% PFOA-b-PS in SC-CO_2 at 338 K and 34.5 MPa. The thickness of the outer PFOA shell remained relatively constant around 76±12 Å.

4. CONCLUDING REMARKS AND FUTURE OUTLOOK

We have described the experimental apparatus and techniques for studying solutions and micellar dispersions in SC-CO_2 using the small angle x-ray and neutron scattering techniques. For solutions these scattering techniques allow us to determine the radius of gyration of the surfactant in solution, its molecular weight, its affinity for SC-CO_2, and its solubility. For dispersions of reverse micelles in SC-CO_2 these techniques allow determination of the size and shape of the reverse micelles and study of the swelling of reverse micelles as material is added to the micelle core. With quantitative calibration, the SAXS technique using our new SAXS pressure cell promises to increase the productivity of this research substantially. Indeed, since acquiring the SAXS data reported here, we have replaced the diamond windows in the cell with a new pair with greatly reduced parasitic scattering (background) in comparison to the originals.

Industry seeks to replace common organic solvents now used in many reaction and separation processes; SC-CO_2 is a potential solvent substitute widely favored by both government and industry. The new surfactants developed by the DeSimone and Beckman groups promise to extend the applicability of SC-CO_2 to many industrial applications involving substances which otherwise would have insufficient solubility SC-CO_2. Still, the currently available surfactants are limited in number and performance. In ongoing work we are coupling our SAXS and SANS scattering studies with complementary molecular simulations in efforts to understand, at a molecular level, what surfactant characteristics lead to improved performance. We hope that superior surfactants for use in SC-CO_2 can be designed and synthesized based on this new level of understanding.

ACKNOWLEDGMENTS

We gratefully acknowledge Joe DeSimone of the University of North Carolina and his co-workers for inspiring this work, for providing sample materials, and for help in performing many of the experiments. We also gratefully acknowledge Roberto Triolo of the University of Palermo and his co-workers for interpretation of the the experiments with micelles. This work was supported by the Divisions of Chemical Sciences and Materials Sciences of the US Department of Energy, by the Laboratory Directed Research Program of ORNL, and by a grant from the National Science Foundation at the University of Tennessee. ORNL is managed by Lockheed Martin Energy Research Corp. for the DOE under Contract No. DE-AC05-96OR22464.

REFERENCES

1. Hendricks, R. W. *J. Appl. Cryst.,* **1978,** 11, 15.

2. Wignall, G. D.; Lin, J. S.; Spooner, S. *J. Appl. Cryst.,* **1990,** 23, 241.

3. Fulton, J. L.; Pfund, D. M.; McClain, J. B.; Romack, T. J.; Maury, E. E.; Combes, J. R.; Capel, M; *Langmuir* **1995,** 11, 4241.

4. Koehler, W. C. *Physica (Utrecht),* **1986,** 137B, 320.

5. Affholter, K. A.; Henderson, S. J.; Wignall, G. D.; Bunick, G. J.; Haufler, R. E.; Compton, R. N. *J. Chem. Phys.* **1994,** 99, 9924.

6. Wignall, G. D.; Bates, F. S. *J. Appl. Cryst.* **1986,** 20, 28.

7. Chillura-Martino, D.; Triolo, R.; McClain, J. B.; Combes, J. R.; Betts, D. E.; Canelas, D. E.; DeSimone, J. M.; Samulski, E. T.; Cochran, H. D.; Londono, J. D.; and Wignall, G. D; *J. Mol. Struct,* **1996,** 383, 3.

8. McClain, J. B.; Betts, D. E.; Canelas, D. E.; Samulski, E. T.; DeSimone, J. M.; Londono, J. D.; Cochran, H. D.; Wignall, G. D; Chillura-Martino, D.; Triolo, R. *Science,* **1996,** 274, 2049.

9. Londono, J. D.; Dharmapurikar, R.; Cochran, H. D.; Wignall, G. D; McClain, J. B.; Combes, J. R.; Betts, D. E.; Canelas, D. E.; DeSimone, J. M.; Samulski, E. T.; Chillura-Martino, D.; Triolo, R. *J. Appl. Cryst.,* in press.

Table I. Results for PFOA Solutions.

MW (g mol^{-1})	A_2 (cm^{3}g^{-2} mol)	R_g (A)
1.0(4)x10^6	0.25(5)x10^{-4}	100(9)
1.1(2)x10^5	0.6(1)x10^{-4}	34(5)

FIGURE CAPTIONS

Figure 1. The 10 m SAXS Facility at ORNL.

Figure 2. ORNL's SAXS Pressure Cell.

Figure 3. ORNL's SANS Pressure Cell.

Figure 4. Zimm plot of PFOA in SC-CO_2.

Figure 5. Determination of MW and A_2.

Figure 6. Pressure limit of solubility of 3 w/v% PFOA at 338K.

Figure 7. 1.9 w/v% PFOA-g-PEO in SC-CO_2 with H_2O and D_2O.

Figure 8. SAXS and SANS for PFOA-b-PS.

Figure 9. Effect of added styrene oligomer.

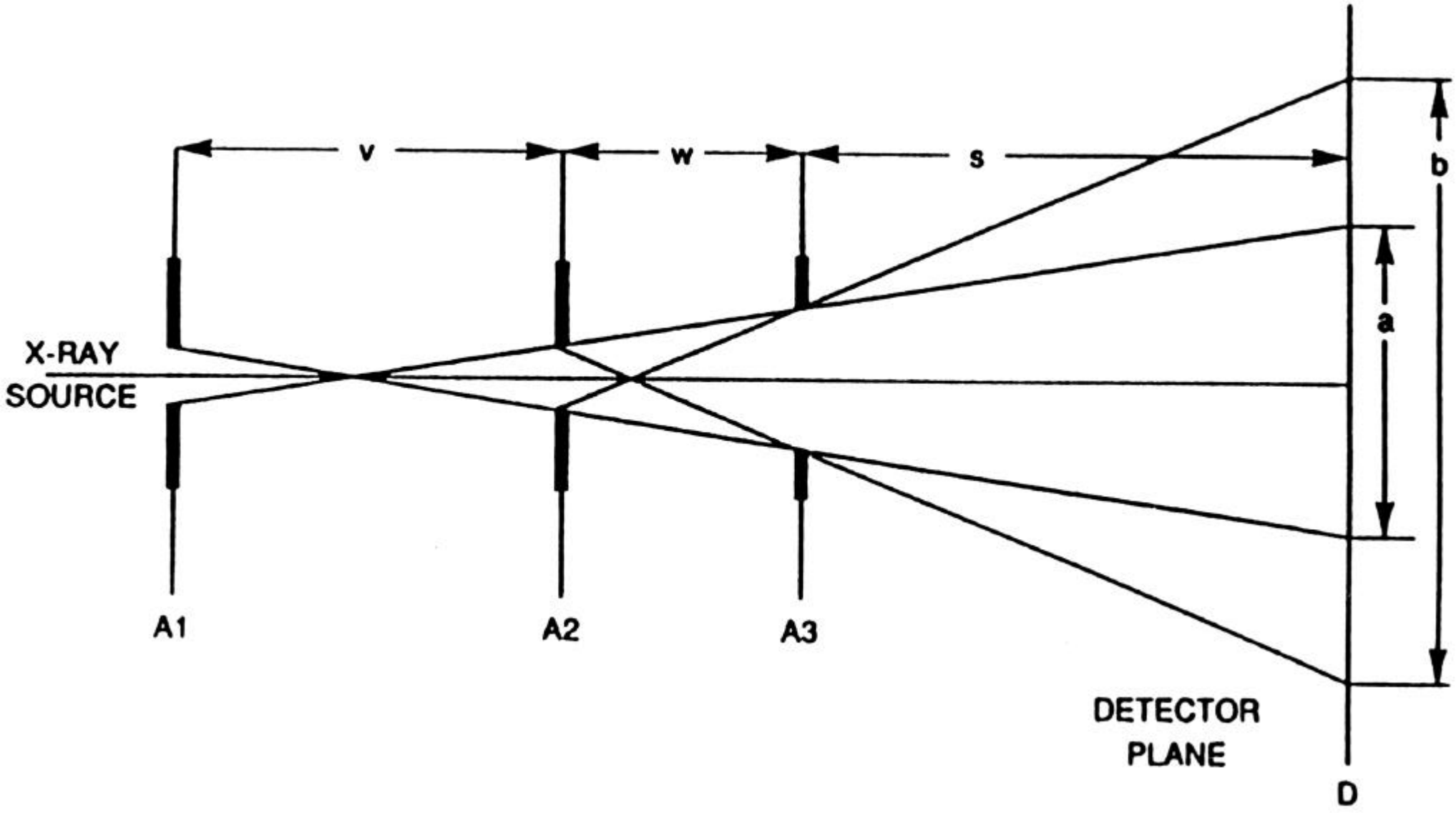
v
w
s
b
a
X-RAY
SOURCE
A1
A2
A3
DETECTOR
PLANE
D

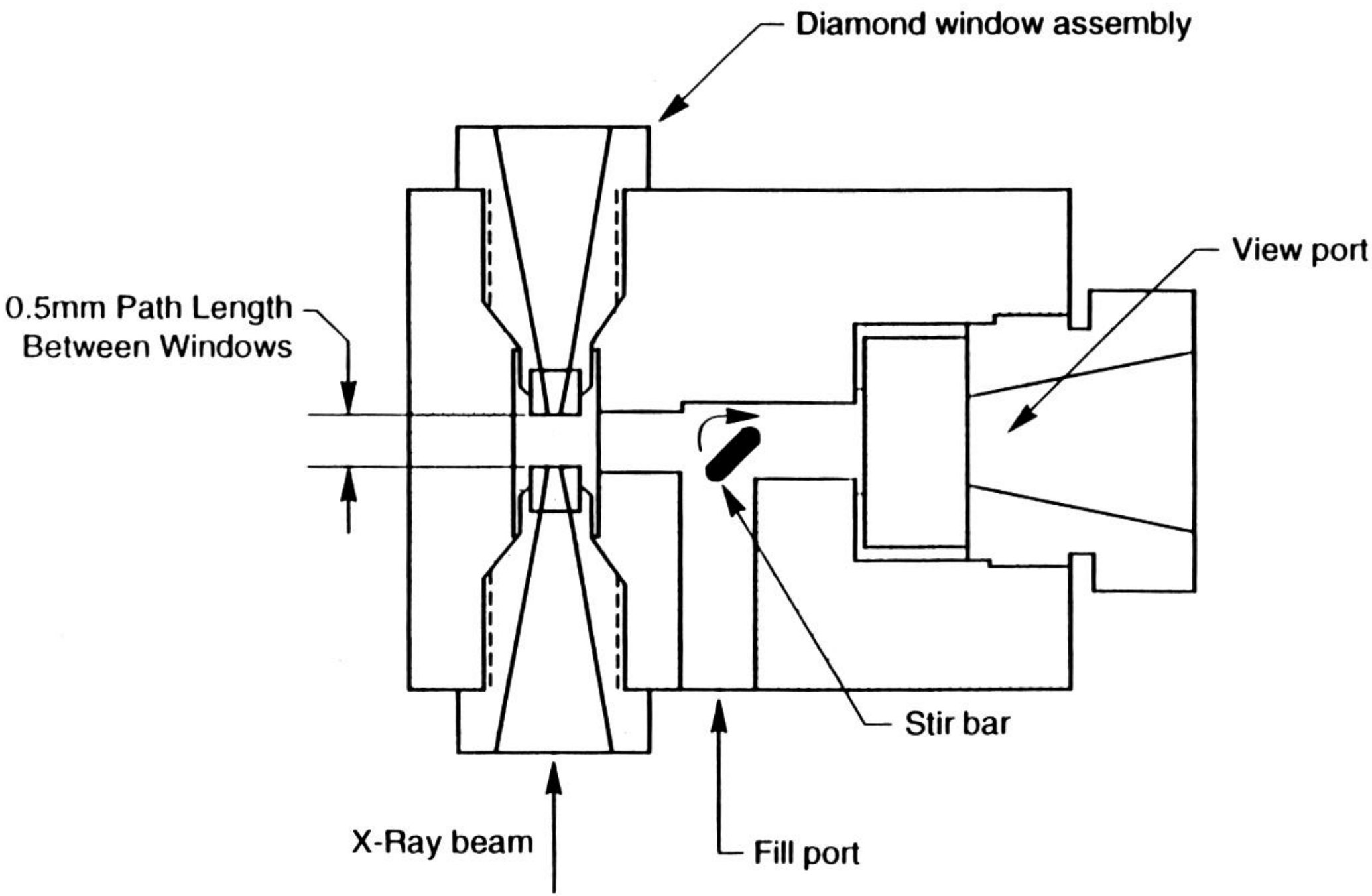
Diamond window assembly
View port
0.5mm Path Length
Between Windows
Stir bar
X-Ray beam
Fill port

ORNL DWG 97C-83

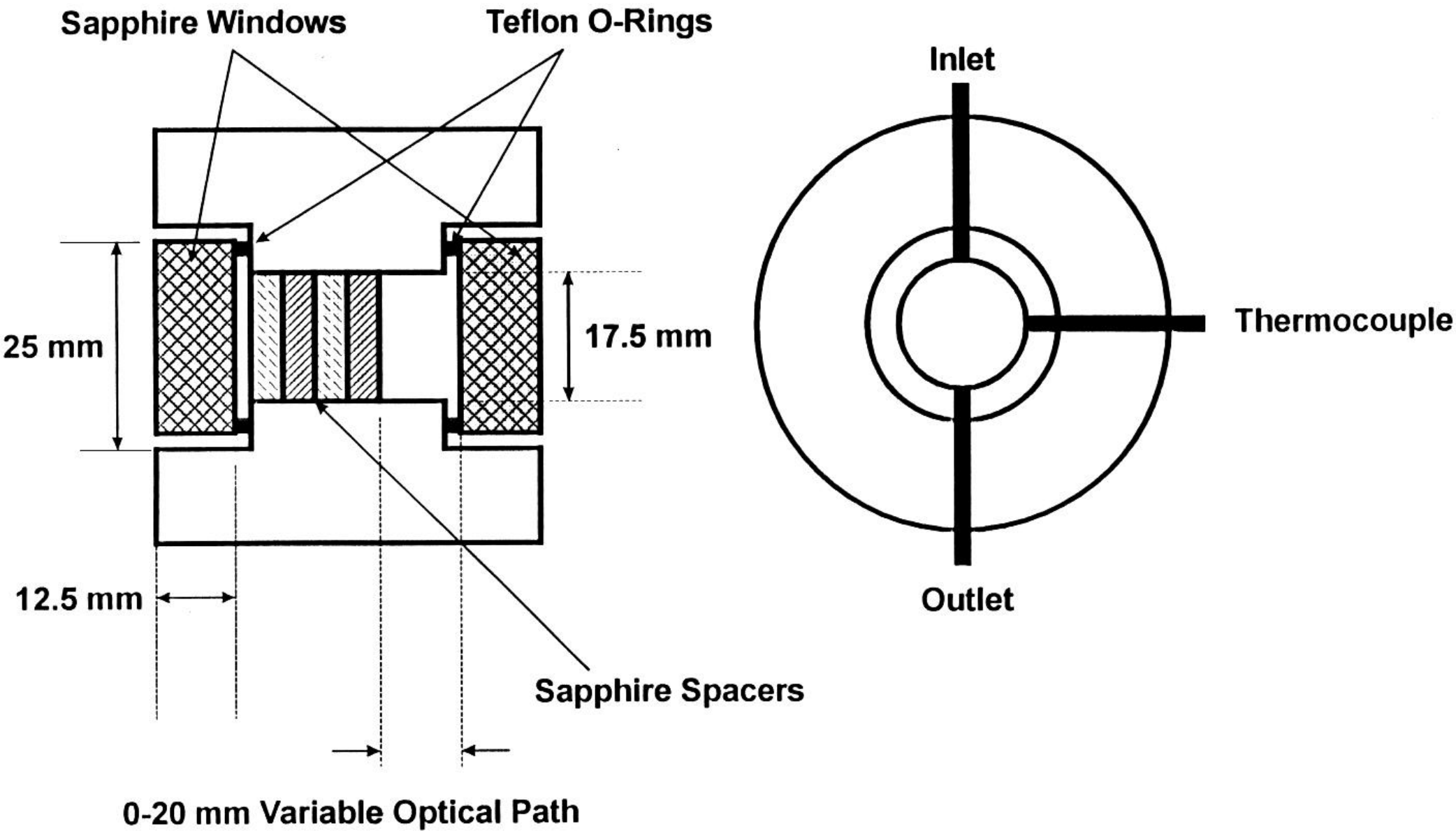

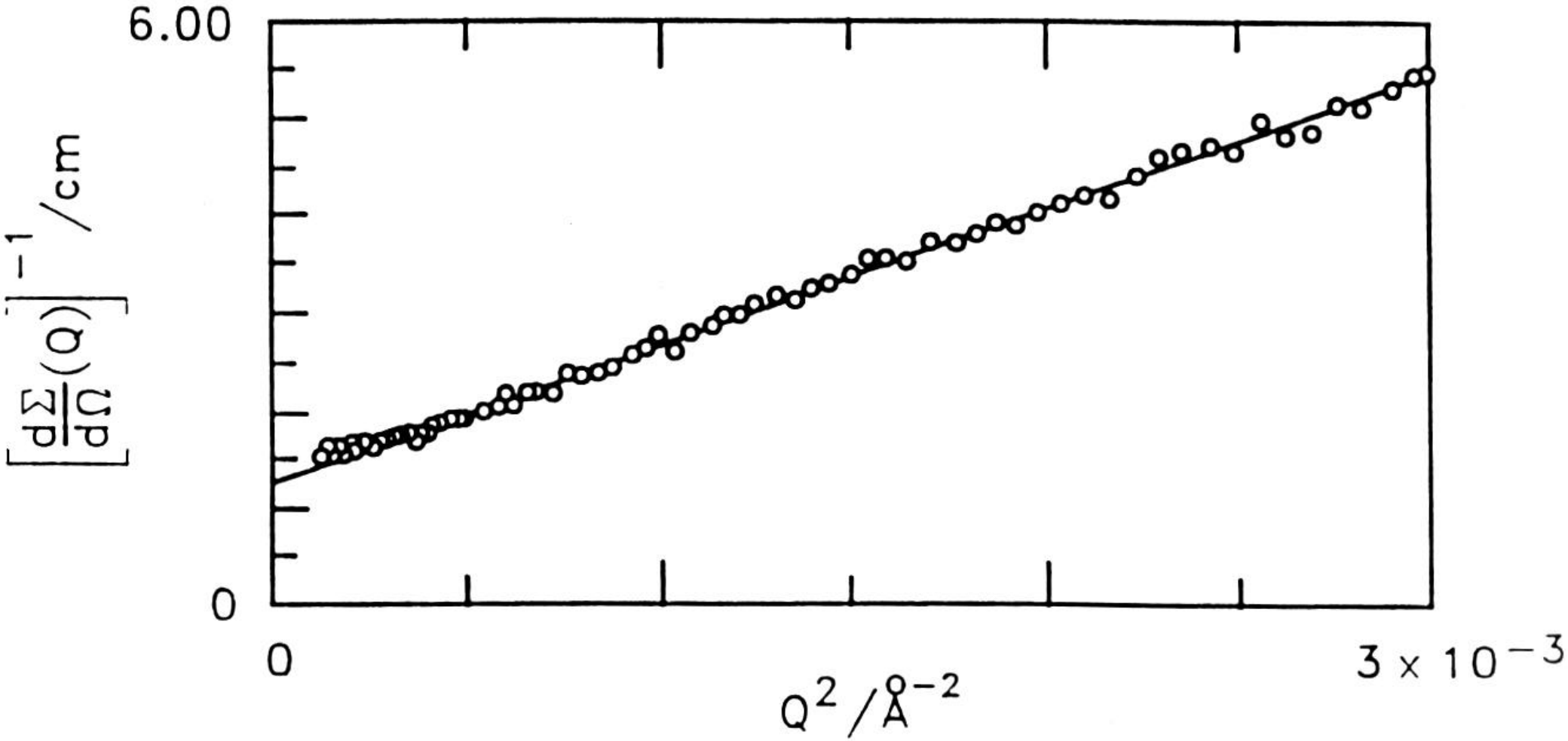
6.00
0
0
3 x 10^-3
Q^2 /Å^-2
[dΣ/dΩ(Q)]^-1 /cm

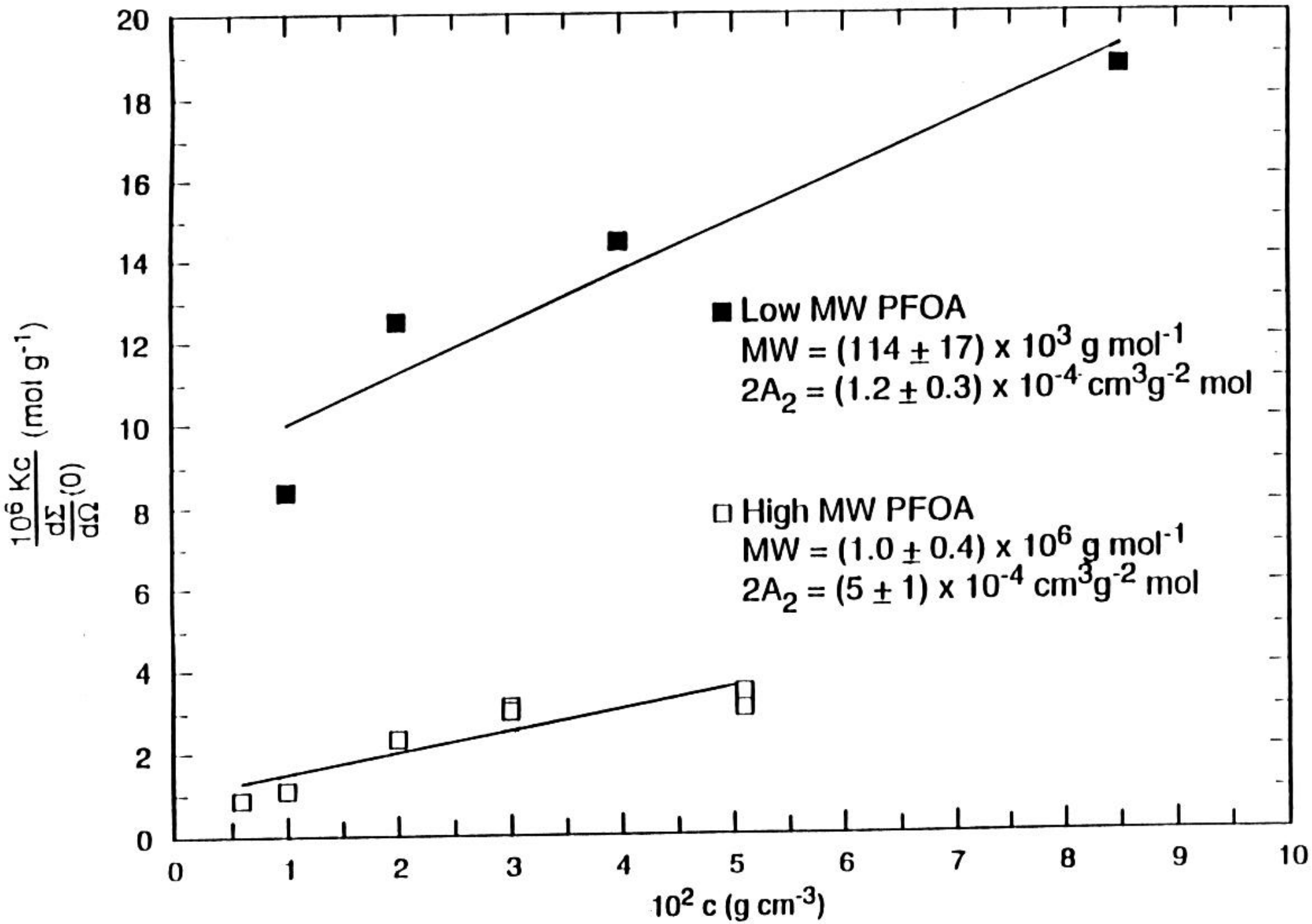
Low MW PFOA
MW = (114 ± 17) x 10^3 g mol^-1
2A2 = (1.2 ± 0.3) x 10^-4 cm^3g^-2 mol
High MW PFOA
MW = (1.0 ± 0.4) x 10^6 g mol^-1
2A2 = (5 ± 1) x 10^-4 cm^3g^-2 mol
10^6 Kc / dΣ/dΩ(0) (mol g^-1)
10^2 c (g cm^-3)
0
2
4
6
8
10
12
14
16
18
20
0
1
2
3
4
5
6
7
8
9
10

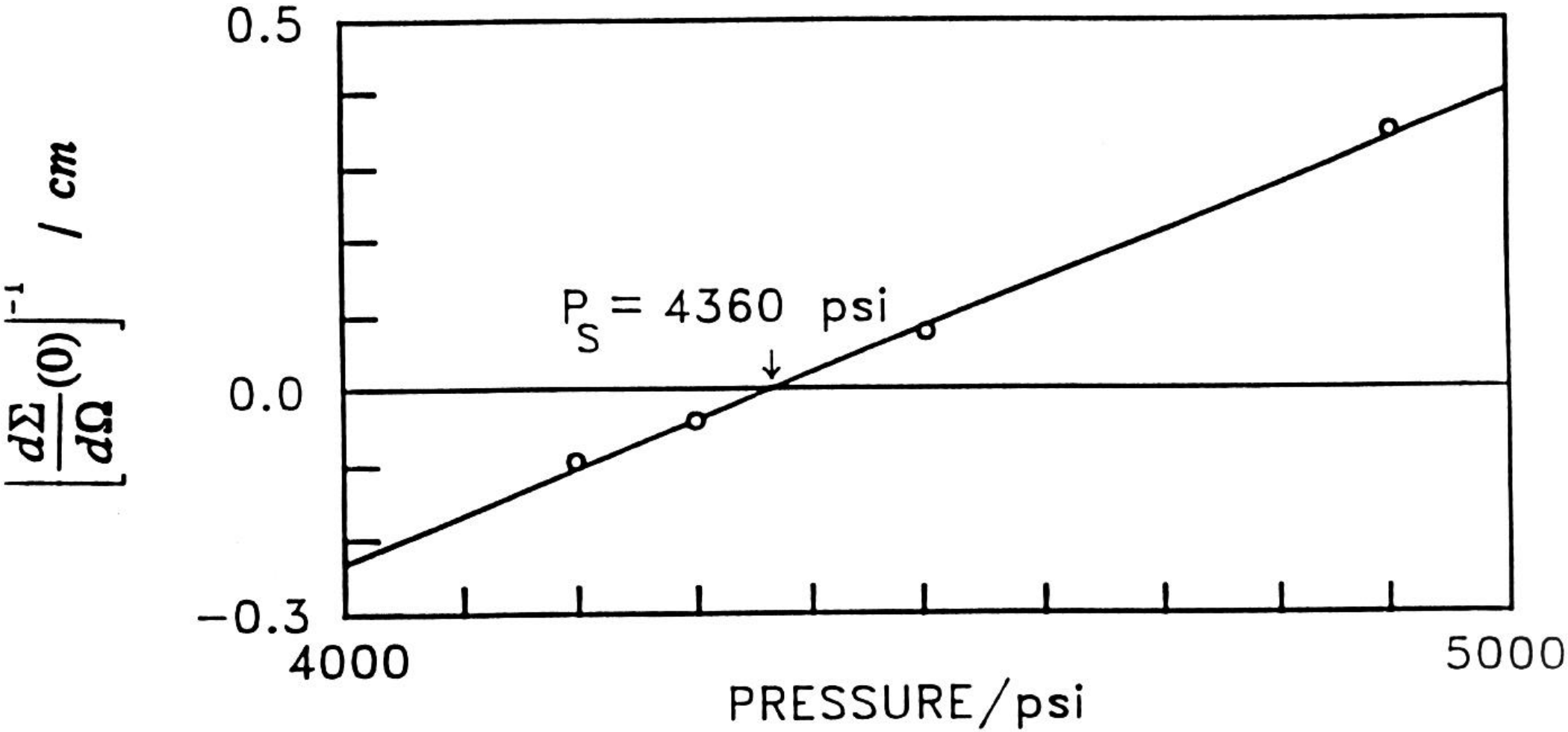
0.5
0.0
−0.3
4000
5000
PRESSURE/psi
P_S = 4360 psi
$\left[\frac{d\Sigma}{d\Omega}(0)\right]^{-1}$ / cm

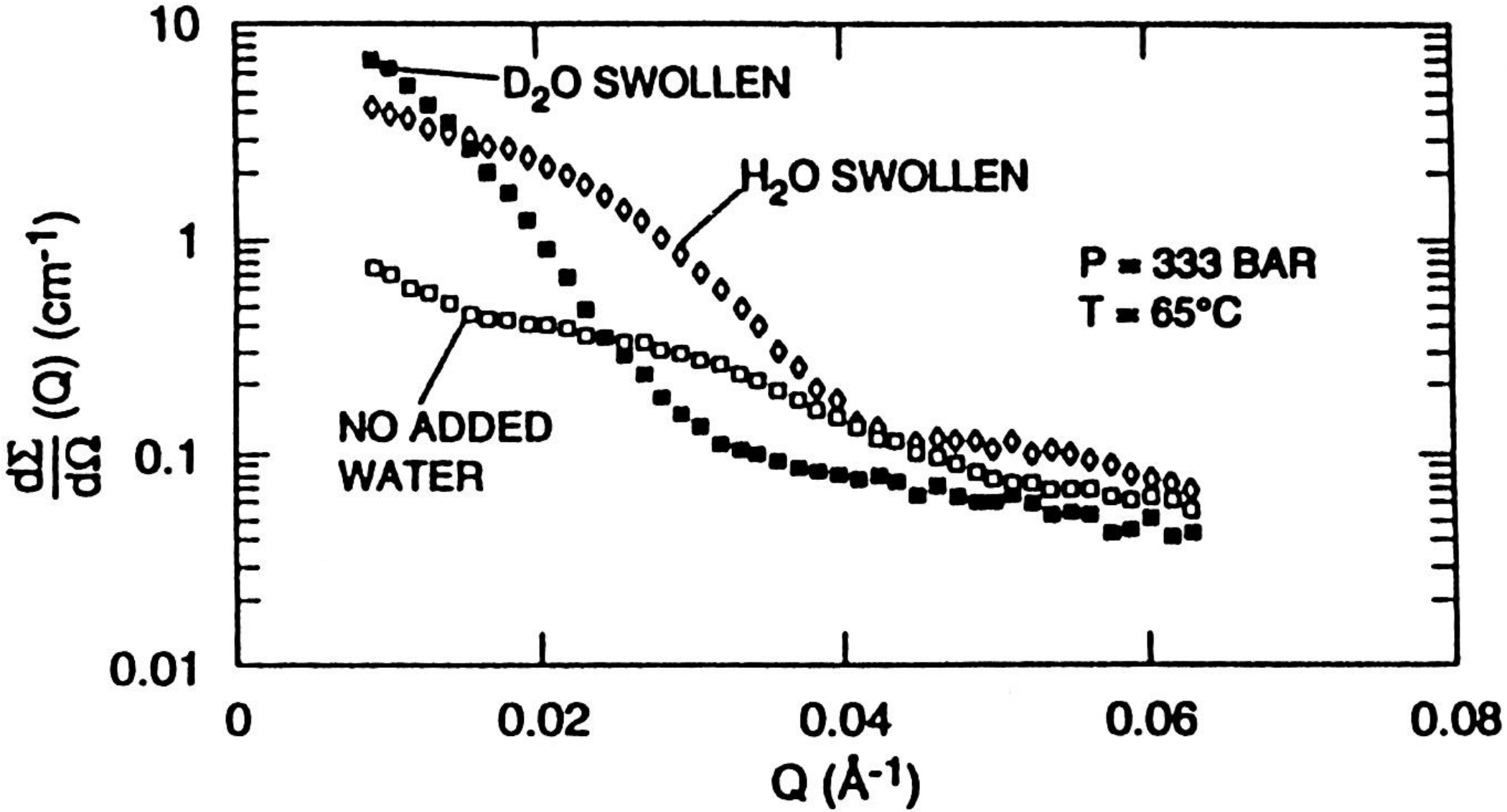
10
1
0.1
0.01
0
0.02
0.04
0.06
0.08
Q (Å-1)
dΣ/dΩ (Q) (cm-1)
D2O SWOLLEN
H2O SWOLLEN
NO ADDED WATER
P = 333 BAR
T = 65°C

ORNL-DWG 96M-3059

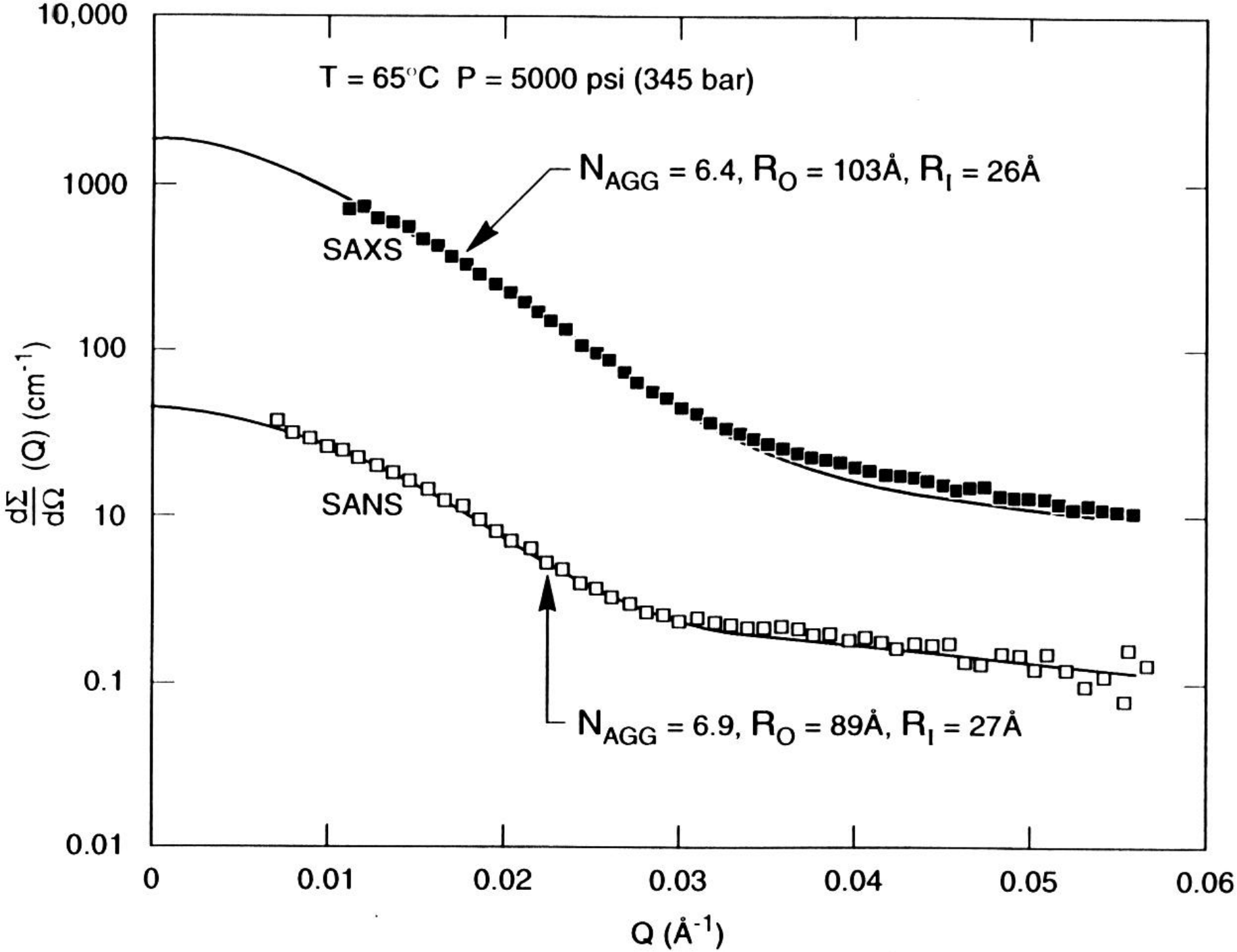

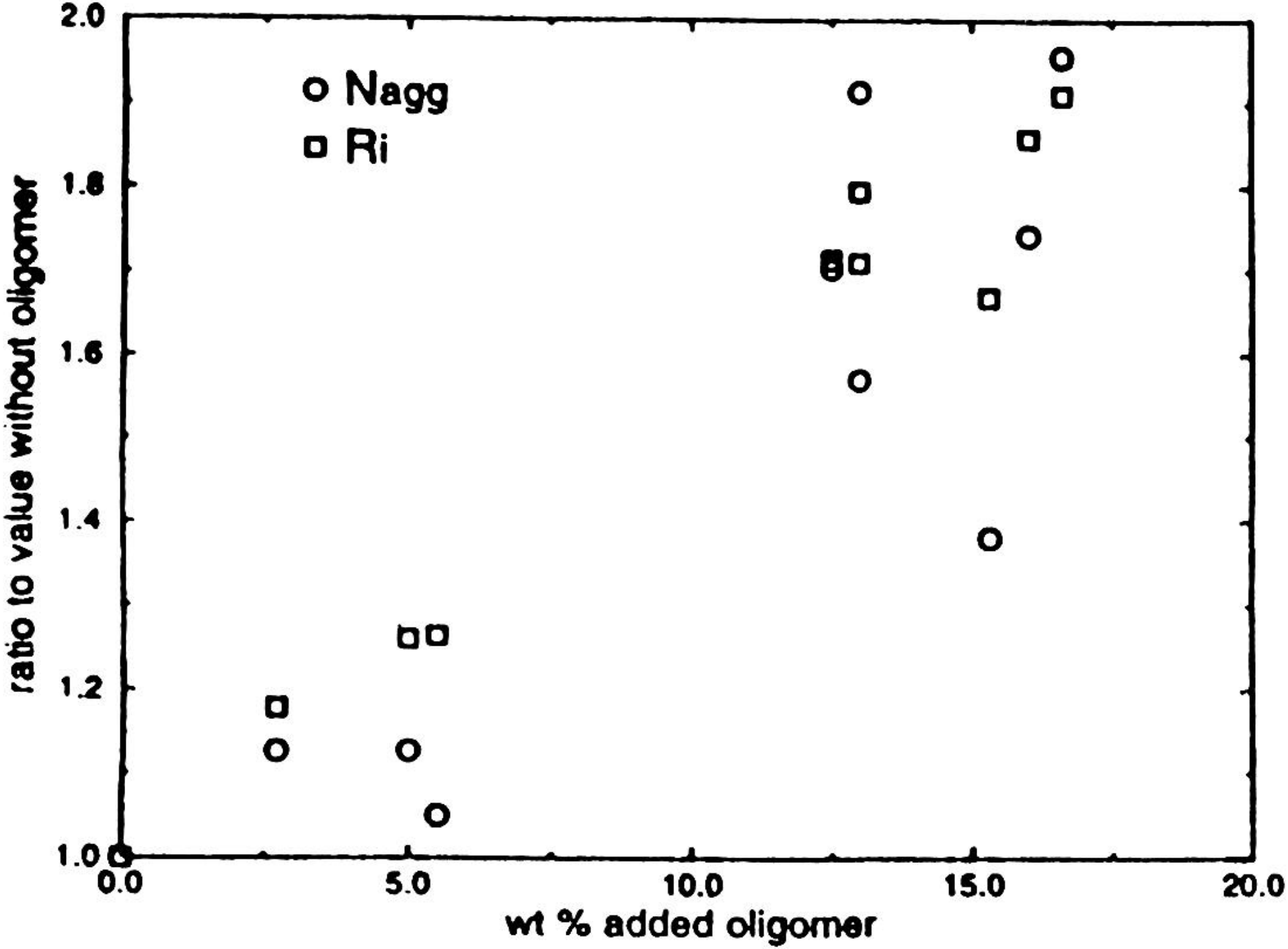
Nagg
Ri
ratio to value without oligomer
2.0
1.8
1.6
1.4
1.2
1.0
0.0
5.0
10.0
15.0
20.0
wt % added oligomer